

# Bose-Hubbard model with a single qubit

R. M. Woloshyn  
TRIUMF, 4004 Wesbrook Mall  
Vancouver, British Columbia, V6T 2A3, Canada

June 14, 2024

## Abstract

The use of a single-qubit parametrized circuit as an *Ansatz* for the variational wave function in the calculation of the ground state energy of a quantum many-body system is demonstrated using the one-dimensional Bose-Hubbard model. Comparison is made to calculations where a classic neural network is used to generate the variational wave function. Computations carried out on IBM Quantum hardware are also presented.

## 1 Introduction

Machine learning based methods are becoming more prevalent in physics. One idea that has gained considerable traction is the use of a neural network as a variational *Ansatz* for many-body systems [1] with applications in condensed matter physics [2, 3, 4] and nuclear physics [5, 6, 7]. In particular, neural quantum states were used in [8, 9] to determine the ground state of the Bose-Hubbard model. Zhu *et al.* [10] extended these calculations in a way that allows for determining ground and excited states over a wide range of parameters with only minimal training.

Another recent trend is the exploration of quantum computing for physics research [11, 12]. Relevant here is the synergy between machine learning and quantum computation. In general, where a classical neural network is being used, one may consider replacing it by a quantum circuit. In this note the use of a parametrized quantum circuit in lieu of the classic neural networks of Refs. [8, 9, 10] for the Bose-Hubbard model is discussed.

In Ref. [13], Pérez-Salinas *et al.* proposed a universal quantum classifier, which, with data multiplexing and re-uploading [14], uses only one qubit. This idea was motivated by the observation that in a classical neural network all features are input into all nodes while in typical quantum neural networks [15, 16] each feature is encoded and first processed by a separate qubit. Using data re-uploading with a single qubit, loading the features in a way more analogous to that of a neural network could be achieved. In a subsequent paper [17], this notion was formalized in the Quantum UAT, a quantum version of the Universal

Approximation Theorem [18, 19] for classical neural networks. A circuit with two parametrized rotation gates acting on a single qubit for implementing the Quantum UAT was presented. In this work, the circuits of [13, 17] are not used as classifiers as originally proposed, but as variational *Ansätze* which are trained to generate the ground state wave function of the one-dimensional Bose-Hubbard model.

Sect. 2 introduces the Bose-Hubbard model and, for comparison to subsequent quantum computations, a variational calculation using a classical neural network for the wave function is presented. The calculation is done in the Fock state basis for a model with six sites and five bosons. This matches the one-dimensional calculation done by Zhu *et al.* [10]. In this section we also discuss how to use the symmetries of the ground state to reduce the size of the required basis to something more suitable for the quantum computation.

Quantum computations, using a classical computer to simulate an ideal quantum device, are presented in Sect. 3. Two different circuits are considered: the compressed scheme (Fig. 2(b) in [13]) and the universal quantum approximant from [17]. Calculations are carried out at a few benchmark points. The results clearly show convergence toward the exact ground state energies but with an accuracy which is not quite as good as the classical neural network. However, the quantum simulations contain a very small number of parameters compared to the neural network and, to save time, used fewer update steps.

To get some insight into the effect of hardware noise on the single qubit calculations energies were calculated on the IBM Quantum processor `ibm_brisbane`. The results, without any error mitigation, are presented in Sect. 4

The wave function of the Bose-Hubbard model is real but, in general, one may have to deal with a complex wave function. The Appendix demonstrates how to do this using a deformation of the Bose-Hubbard Hamiltonian with a complex phase in the hopping term.

## 2 Bose-Hubbard model

The Hamiltonian for the Bose-Hubbard model, in the absence of an external and chemical potential, is

$$\mathcal{H} = -t \sum_{\langle i,j \rangle} a_i^\dagger a_j + \frac{U}{2} \sum_i n_i(n_i - 1), \quad (1)$$

where  $a_i^\dagger$  and  $a_i$  are the usual boson creation and annihilation operators with the commutation relation  $[a_i, a_j] = \delta_{ij}$  and  $n_i = a_i^\dagger a_i$  is the number operator at site  $i$ . Periodic boundary conditions are imposed.

Calculations are typically done in the basis of Fock states which enumerate the number of bosons at each site. For  $N$  bosons and  $M$  sites the total number of Fock states is

$$\binom{N + M - 1}{N}.$$

U	Exact	Neural network full basis	Neural network reduced basis
2	-7.54752	-7.54750	-7.54747
5	-5.46241	-5.46236	-5.46233
8	-4.37439	-4.37439	-4.37388

Table 1: Results for the ground state energy for different values of the on-site interaction energy  $U$  at  $t = 1$  using a neural network variational *Ansatz*. Results of exact diagonalization are also shown.

The basis size grows exponentially so, for example, in [9] with 8 sites, the basis is too large for an exact evaluation of the energy. Monte Carlo sampling was used to approximate the expectation value of the Hamiltonian. For the present calculation, following [10] with, with  $M = 6$  and  $N = 5$  the number of Fock states is only 252 so the full basis can be used.

The ground state energy is calculated using a variational method and a neural network is used to determine the coefficients of a Fock state expansion of the wave function [9, 10]. The network parameters are the variational parameters that are tuned to minimize the energy. In machine learning terminology, the site occupation numbers of the Fock states are the features and Fock states comprise the data sample. Note that unlike a typical machine learning classification problem, mini-batches are not used here.

The neural network used here is comprised an input layer with 6 inputs corresponding to the number of sites, two hidden layers with 64 and 32 nodes respectively and a linear output layer with a single output. Each hidden layer has a Tanh activation. The total number of parameters is 2560. Following [9], the network input is pre-processed by subtracting the average occupancy  $N/M$  from the individual Fock state occupation values. The wave function coefficients are calculated by taking the exponential of the network output. This ensures that all coefficients have the same sign as in the true wave function.

The network was implemented using Pytorch [20]. The Adam optimizer with learning rate of 0.02 was used. Training runs consisted of 1500 update steps using the full sample of 252 basis states. Results are shown in Table 1 along with the results from exact diagonalization.

The full Fock state wave function contains many redundant values. Due to translation invariance with periodic boundary conditions, Fock states whose occupation numbers are cyclic permutations of each other have the same weight. By using a basis of composite states consisting of the 6 states related by translation the basis size can be reduced from 252 to 42. Furthermore, in the ground state, Fock states whose occupation numbers are related by a parity transformation, for example,  $|012011\rangle$  and  $|110210\rangle$ , have the same coefficient. This can be used to reduce the the basis size, from 42 to 26 in the present case. Neural network variational results using the 26 states basis are given in the last column of Table 1. This is the basis that will be used in the quantum computation. Note that it can only be use to get ground state since in excited states not all

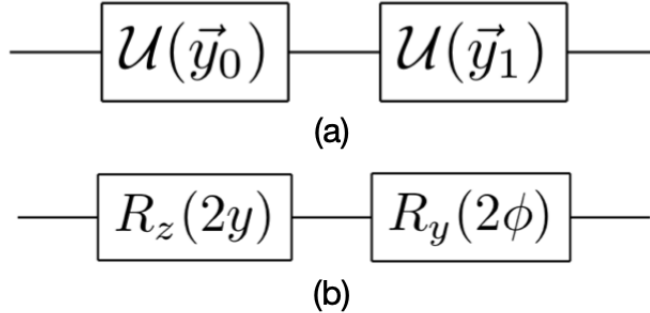


Figure 1: One-qubit circuits: (a) One layer of the compressed scheme circuit. The gate  $\mathcal{U}$  is a general single-qubit unitary. The 6 features  $\vec{x}$  are divided into 2 triplets. There are 7 parameters per layer, 6 weights  $\vec{\omega}$  and 1 bias  $b$ , the same for all triplets. (b) Implementation of the fundamental UAT gate of [17]. There are 8 parameters per layer, 6 weights  $\vec{\omega}$  and 1 bias  $b$  plus a rotation angle  $\phi$ .

wave function coefficients have the same sign so the composite states used here will not be applicable.

### 3 Quantum computation with a single qubit

A variety of quantum counterparts to classical neural networks have been proposed. For a review see [15, 16]. In the typical architecture, each feature is loaded in a separate qubit and processing follows. The circuits used here differ in two essential ways. First, multiple data are loaded in the same input channel. Secondly, loading and processing the data take place in the same quantum gates.

The two different circuits used in this work are shown in Fig. 1. Fig. 1(a) is based on the universal quantum classifier using the compressed scheme proposed in [13]. The input data are grouped in triplets  $\vec{x}$  and combined with variational parameters  $(\vec{\omega}, b)$  to form the arguments of general unitary operators. In the present application, with six input features, a layer of this circuit has two unitary operators with arguments given by

$$\vec{y}_j = [b + \omega_{3j}x_{3j}, b + \omega_{3j+1}x_{3j+1}, b + \omega_{3j+2}x_{3j+2}], j = 0, 1. \quad (2)$$

Data are re-uploaded using multiple layers of the basic circuit with each layer having seven parameters.

An alternative circuit QUAT, uses multiple layers of the fundamental UAT gate [17] shown in Fig. 1(b). All features  $\vec{X}$  are combined into a single variable given by

$$y = \vec{\omega} \cdot \vec{X} + b, \quad (3)$$

Layers	Compressed scheme	QUAT circuit
3	-5.40019	-5.02048
4	-5.45876	-5.35662
5	-5.45396	-5.39576
6	-5.46048	-5.46175

Table 2: Variational energy estimate after 1200 training steps with model parameters  $t = 1$  and  $U = 5$  for different numbers of layers of the basic circuits in Fig. 1.

U	Exact	Neural network reduced basis	Quantum compressed	Quantum QUAT
2	-7.54752	-7.54747	-7.54750	-7.54751
5	-5.46241	-5.46233	-5.46048	-5.46175
8	-4.37439	-4.37388	-4.36807	-4.31310

Table 3: Comparison of the variational energy estimate from quantum simulation with exact and neural network values at  $t = 1$  and different values of  $U$ . The quantum simulations used 6 layers and were terminated after 1200 update steps.

The rotation gate  $R_y(2\phi)$  is meant to play a role like the activation function of a neural network. With six input features there are eight parameters per layer.

The reduced 26-state basis is used in the quantum calculations. A single Fock state was chosen from each of 26 classes making up the composite basis states to serve as a representative input sample. For each of these, the average value of the qubit in the computational basis after application of the circuit is used as the weight of the corresponding basis state in the variational wave function. The approach here is a hybrid one, the calculation of wave function weights is quantum, the energy calculation and minimization are classical.

To determine the efficacy of the single qubit circuits as variational *Ansatz* computations were done on a classical computer simulating an ideal quantum computer. In other words, there was no quantum measurement uncertainty and no hardware noise. These issues will be discussed briefly in the next section. The PennyLane quantum programming framework [21] was used to implement the simulation. The Adam optimizer, running on a classical computer, was used for energy minimization.

The first step is to determine if the single qubit *Ansatz* will actually work and how many layers may be required. The loss, defined as the exact ground state energy minus the variational estimate, as a function of upgrade step using different numbers of the compressed scheme circuits for the model parameters  $t = 1$  and  $U = 5$ . The number of parameters increases from 21 with 3 layers to 42 with 6 layers. Table 2 shows how the estimated energy varies with number of layers for both types of circuits.

Finally, the results of quantum simulation are compared to exact and neural

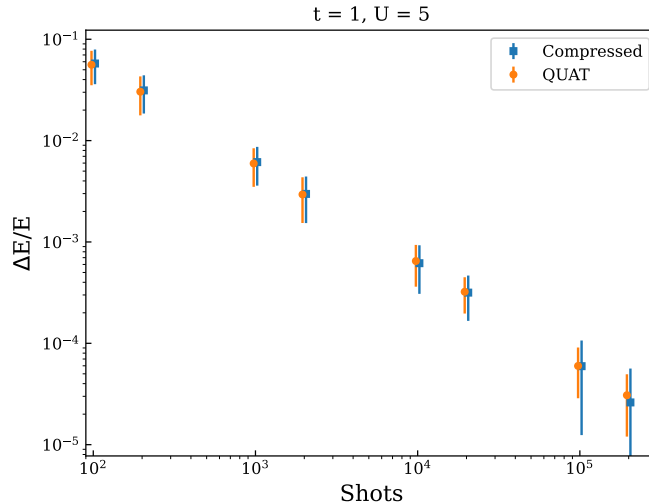


Figure 2: Fractional energy difference between an ideal simulation and a simulation with finite shots. Symbols are median values from 100 trials. Error bars reflect the standard deviation of the trial distribution.

network values for the three benchmark model parameter sets in Table 3. The results using a single qubit are very reasonable although slightly less accurate than the neural network. However, it should be kept in mind that the quantum circuits have about 50 times fewer parameters than the neural networks and there may still be room to improve the results by increasing training and tuning the optimizer.

## 4 Noisy simulation

Since access to quantum resources was limited, it was not feasible to carry out training on a real quantum device. However, it is possible to gain some insight into the performance of the circuits by calculating the energy using trained circuits on a real device. The first step is to determine how the number of measurements (shots) affects the calculation of the wave function and hence the value of the energy. This was done on the quantum simulator without hardware noise. Fig. 2 shows the difference between the energy calculated using a finite number of shots and the ideal value (essentially infinite shots) as fraction of the ideal energy. The results were obtained by taking the median of 100 trials for each value of the shots. The error bars reflect the standard deviation of the distribution of trial values. A practical limit for an actual quantum computation is about 20,000 shots where  $\Delta E/E$  is below  $10^{-3}$ .

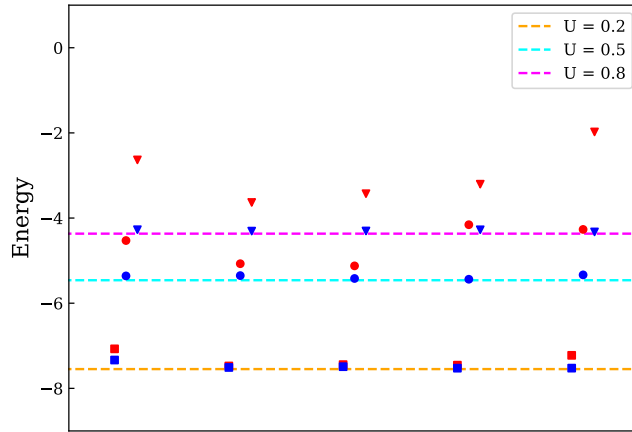


Figure 3: Five ground state energies using wave functions computed in a single run on `ibm_brisbane` with (blue symbols) and without (red symbols) readout error correction using the compressed scheme circuit. Triangles, circles and squares correspond to  $U = 0.2, 0.5$  and  $0.8$  respectively. The ideal hardware error-free results are shown by dashed lines

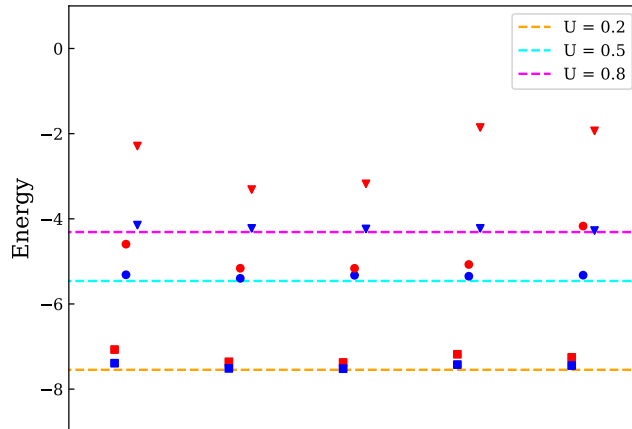


Figure 4: Five ground state energies using wave functions computed in a single run on `ibm_brisbane` with (blue symbols) and without (red symbols) readout error correction using the QUAT circuit. Triangles, circles and squares correspond to  $U = 0.2, 0.5$  and  $0.8$  respectively. The ideal hardware error-free results are shown by dashed lines

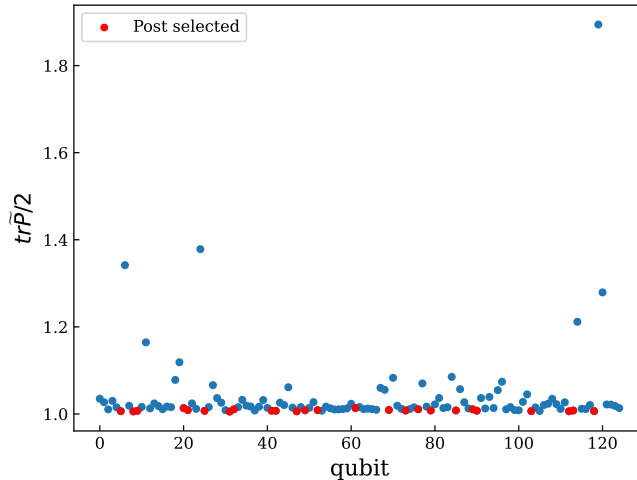


Figure 5: The readout figure of merit  $\text{tr}\tilde{P}/2$  (see Appendix A) for 125 qubits (blue symbols). The selected qubits are shown in red.

The final step is to calculate energies on a real quantum device. This was done on IBM Quantum resources using the Qiskit toolkit [22].

The ground state wave function with the reduced Hamiltonian contains 26 terms. Since normalization of the wave function provides one constraint, 25 coefficients need to be calculated. This is done using 25 qubits each one getting a different Fock state configuration as input and computing the corresponding wave function coefficient. Since the `ibm_brisbane` processor has 127 qubits five wave functions can be computed at once. The five resulting ground state energies, using 20,000 shots per measurement and without any error mitigation, are plotted with red symbols in Figs. 3 and 4. The ideal hardware error-free results are shown by dashed lines.

In most quantum computations, two-qubit gates are the dominant contributors to hardware noise. Since such gates are absent in this calculation one might expect readout errors to be the main source of the discrepancy between the red symbols in Figs. 3 and 4 and the error-free values. How to estimate readout error correction factors is discussed in Appendix A. Calibration runs were done and applying correction factors gives results shown by the blue symbols in Figs. 3 and 4.

It is possible to do better. Fig. 5 shows an example of the readout figure of merit  $\text{tr}\tilde{P}/2$  (see Appendix A) for all 125 qubits. A value closer to one means smaller readout error. Having a measurement of each wave function coefficient on five qubits one can postselect the coefficient calculated on the qubit having the best figure of merit. The selected qubits are shown in red symbols. The results using postselected qubits with and without readout error correction are



Compressed			
U	Error-free	Uncorrected	Corrected
2	-7.5474	-7.3815	-7.3697
5	-5.4603	-5.3665	-5.3864
8	-4.3665	-4.1936	-4.3167
QUAT			
	Error-free	Uncorrected	Corrected
2	-7.5461	-7.4059	-7.3962
5	-5.4600	-5.3425	-5.3741
8	-4.3111	-4.1242	-4.2697

Table 4: Ground state energy using post selected qubits without and with readout error correction applied. The value computed using a simulator without hardware error is also shown.

shown in Table 4. As expected, with postselection the readout error correction is quite small.

It is probably possible to do even better by preselecting the qubits on which to calculate the 25 coefficients. This is left as an exercise for the reader.

## 5 Summary

Single-qubit parametrized circuits were used for constructing the variational wave function of a one-dimensional Bose-Hubbard model. The circuits, which feature data re-uploading, were originally proposed for use classification problems [13, 17]. It is shown here, that just as variational quantum states are constructed with neural networks, one-qubit circuits can also serve as variational *Ansätze* [1].

The circuits were trained by minimizing the ground state energy using an ideal quantum simulator implemented in PennyLane [21]. The results obtained were comparable, but slightly less accurate than those from a neural network variational wave function utilizing about 50 times more parameters.

After training, the circuits were run on `ibm_brisbane`. Only readout error mitigation was applied. Typically the results were within a couple percent of the error-free values. For future work one may try to remove the remaining discrepancy by a careful calibration and preselection of qubits and, for example, zero-noise extrapolation [23] with unitary folding [24] to deal with gate errors<sup>1</sup>.

---

<sup>1</sup>Of course, the ultimate in error mitigation would be to use an error-correcting logical qubit. Since, in principle, only one is required this may be feasible in the not-too-distant future.

## Acknowledgment

Thanks to Olivia Di Matteo for helpful comments.

We acknowledge the use of IBM Quantum resources in carrying out this work. The views expressed are those of the author, and do not reflect the official policy or position of IBM or the IBM Quantum team

TRIUMF receives federal funding via a contribution agreement with the National Research Council of Canada.

## Appendix A

A brief description of the readout error correction is given here. Let  $p_{ij}$  denote the probability that a qubit in state  $j = \{0, 1\}$  is recorded to be in state  $i$ . Then

$$N^O = \begin{pmatrix} N_0^O \\ N_1^O \end{pmatrix} = \begin{pmatrix} p_{00} & p_{01} \\ p_{10} & p_{11} \end{pmatrix} \begin{pmatrix} N_0^T \\ N_1^T \end{pmatrix} = PN^T$$

where  $N^T$  and  $N^O$  denote the number of true and observed values respectively in a set of  $N_0 + N_1$  measurements. The inverse of  $P$ , which will be denoted as  $\tilde{P}$ , can then be used to map observed values to true values.

To estimate  $P$ , two calibration runs are done. One to prepare the qubit in state  $|0\rangle$  and measure and the other to prepare  $|1\rangle$  and measure. In this work, the calibration runs consisted of 20,000 shots, the same as the data-taking runs. All 125 qubits used for data-taking were calibrated in the same run.

Generically, the diagonal elements of  $\tilde{P}$  are greater than or equal to 1. A value of 1 would indicate that there is no readout error. Therefore,  $\text{tr}\tilde{P}/2$  is used as figure of merit for selecting qubits with small readout error.

## Appendix B

The wave function of the Bose-Hubbard model has only real coefficients but for other models, complex coefficients may appear. To deal with this possibility neural networks with two linear outputs  $(x_0, x_1)$  are used. The wave function weight is then taken to be  $e^{x_0 + ix_1}$ , *i.e.*, one output provides the magnitude and the other one, the phase [8, 9, 10].

To generate complex coefficients with the single-qubit *Ansatz* one can prepare the circuit twice for each basis state. For example, once for the measurement of the expectation value  $\langle\sigma_z\rangle$  and then for  $\langle\sigma_x\rangle$ . Then for the magnitude of the wave function coefficient use  $(1 + \langle\sigma_z\rangle)/2$  with  $e^{i\pi\langle\sigma_x\rangle}$  as the phase<sup>2</sup>.

To test a variational calculation with a complex wave function a deformation of the Bose-Hubbard Hamiltonian in the reduced basis was made by introducing phases  $e^{\pm i\varphi}$  in the hopping terms preserving hermiticity. With  $t = 1, U = 5$  and  $\varphi = \pi/2$ , exact diagonalization of the Hamiltonian gives a ground state energy of  $-4.6590$  while a variational calculation with a neural network using the same

---

<sup>2</sup>In practice one should test other combinations of measurements to optimize convergence.

two-hidden-layer architecture as in Sect. 2 (but with two outputs), gave an energy of -4.6583.

One qubit circuits were used as described above. Convergence was considerably slower compared to the case with of a real wave function described in Sect. 3. To overcome this, the number of layers was increased to 8 and the number of update steps was increased. The resulting energies were -4.6431 for the compressed scheme circuit but only -4.5598 for the QUAT circuit. There may be scope for further optimization but it was not pursued here.

## References

- [1] G. Carleo and M. Troyer, *Science* **355**, 602 (2017).
- [2] Y. Nomura, A. S. Darmawan, Y. Yamaji and M. Imada, *Phys. Rev. B* **96**, 205152 (2017).
- [3] K. Choo, A. Mezzacapo and G. Carleo, *Nature Communications* **11**, 2368 (2020).
- [4] N. Yoshioka, W. Mizukami and F. Nori, *Communications Physics* **4**, 106 (2021).
- [5] J. Keeble and A. Rios, *Physics Letters B* **809**, 135743 (2020).
- [6] C. Adams, G. Carleo, A. Lovato and N. Rocco, *Phys. Rev. Lett.* **127**, 022502 (2021).
- [7] A. Gnech *et al.*, *Few-Body Systems* **63**, 7 (2021).
- [8] H. Saito, *Journal of the Physical Society of Japan* **86**, 093001 (2017).
- [9] H. Saito and M. Kato, *Journal of the Physical Society of Japan* **87**, 014001 (2018).
- [10] Z. Zhu, M. Mattheakis, W. Pan and E. Kaxiras, *Phys. Rev. Res.* **5**, 043084 (2023).
- [11] J. E. García-Ramos, A. Sáiz, J. M. Arias, L. Lamata and P. Pérez-Fernández, *Nuclear physics in the era of quantum computing and quantum machine learning*, 2023, [arXiv:2307.07332].
- [12] A. D. Meglio *et al.*, *Quantum computing for high-energy physics: State of the art and challenges. summary of the qc4hep working group*, 2023, [arXiv:2307.03236].
- [13] A. Pérez-Salinas, A. Cervera-Lierta, E. Gil-Fuster and J. I. Latorre, *Quantum* **4**, 226 (2020).
- [14] J. Gil Vidal and D. O. Theis, *Input redundancy for parameterized quantum circuits*, 2020, [arXiv:1901.11434].

- [15] Y. Kwak, W. J. Yun, S. Jung and J. Kim, Quantum neural networks: Concepts, applications, and challenges, 2021, [arXiv:2108.01468].
- [16] R. Zhao and S. Wang, A review of quantum neural networks: Methods, models, dilemma, 2021, [arXiv:2109.01840].
- [17] A. Pérez-Salinas, D. López-Núñez, A. García-Sáez, P. Forn-Díaz and J. I. Latorre, *Phys. Rev. A* **104**, 012405 (2021).
- [18] G. Cybenko, *Mathematics of Control, Signals and Systems* **2**, 303 (1989).
- [19] K. Hornik, *Neural Networks* **4**, 251 (1991).
- [20] A. Paszke *et al.*, Pytorch: An imperative style, high-performance deep learning library, 2019, [arXiv:1912.01703].
- [21] V. Bergholm *et al.*, PennyLane: Automatic differentiation of hybrid quantum-classical computations, 2022, [arXiv:1811.04968].
- [22] Qiskit contributors, Qiskit: An open-source framework for quantum computing, 2023.
- [23] K. Temme, S. Bravyi and J. M. Gambetta, *Phys. Rev. Lett.* **119**, 180509 (2017).
- [24] T. Giurgica-Tiron, Y. Hindy, R. LaRose, A. Mari and W. J. Zeng, Digital zero noise extrapolation for quantum error mitigation, in *2020 IEEE International Conference on Quantum Computing and Engineering (QCE)*, pp. 306–316, 2020.